Vol 17 No 9, September 2008
1674-1056/2008/17(09)/3306-07

Chinese Physics B

© 2008 Chin. Phys. Soc.
and IOP Publishing Ltd

Quantum coherent effects in multi-Zeeman-sublevel atomic systems*

Dong Ya-Bin(董雅宾)[a)†], Gao Jiang-Rui(郜江瑞)[a)b)], and Dong You-Er(董有尔)[a)]

[a)] *Department of Physics, Shanxi University, Taiyuan* 030006, *China*
[b)] *State Key Laboratory of Quantum Optics and Quantum Optics Devices, Institute of Opto-Electronics, Shanxi University, Taiyuan* 030006, *China*

(Received 23 January 2008; revised manuscript received 5 March 2008)

This paper reports the experimental results on electromagnetically induced absorption (EIA) spectra observed in the system which does not satisfy completely the conditions given by Lezama *et al* [1999 *Phys. Rev.* A **59** 4732]. EIA signals on the transitions in the Cs D_2 line are able to be observed, where $F_g \leftrightarrow F_e = F_g - 1$ as open systems. Theoretical model of Lezama *et al* is good for the case $F_g \leftrightarrow F_e = F_g + 1$, considering spontaneous transfer of atomic coherences or populations this model is not able to explain our experimental results obtained in the case $F_g \leftrightarrow F_e = F_g - 1$. This paper offers a theoretical model which is able to well explain the case $F_g \leftrightarrow F_e = F_g - 1$. It also uses this theoretical model to explain the split and shift of EIA peaks, which have been obtained in experiments.

Keywords: electromagnetically induced absorption, multi-Zeeman-sublevel
PACC: 3260V, 4225B, 4250

1. Introduction

The properties of atoms and molecules such as absorption, dispersion, and a variety of nonlinear characteristics can be manipulated by the addition of extra electromagnetic fields.[1,2] For examples, an induced transparency was found in an initially absorbing medium, experienced by a weak-probe field, due to the presence of a strong-coupling field on a linked transition.[3,4] Lasers can operate normally without population inversion between levels relevant for the lasing transition.[5,6] Coherent population trapping (CPT),[7,8] large refractive indexes,[9] slow light and storage of quantum information in a coherent media have been achieved.[10,11] More recently, these effects have found potential applications in quantum information system, among which there are quantum computation,[9] the quantum logic gate,[12] quantum switches[13] and quantum interferometric optical lithography,[14] which offer many advantages over conventional ones.

Most of these phenomena have been widely studied in typical Λ-type and V-type three-level or four-level atomic systems (simple models). The experimental demonstrations of these phenomena were often carried out in atoms,[15−17] and the theoretical analysis based on simple models indicates that the foundations of these effects are the atomic coherence and the destructive quantum interference among different transition pathways. However, in real atomic systems, the atomic states usually have complex structure with degenerate Zeeman sublevels which can lead to interesting variations of absorption induced by the competition between electromagnetically induced transparency (EIT) and absorption effects due to the interplay between the dominance of Rabi frequency and multi-Zeeman-sublevel.[18,19] Recently, quantum coherences in the degenerate atomic system have attracted great interests because they exhibit not only the CPT and EIT of the simple three-level system but also electromagnetically induced absorption (EIA) in the absorption spectra. The quantum coherences in the degenerate two-level system were extensively studied both experimentally and theoretically in Akulshin's group,[20−22] who demonstrated that EIA can occur in the degenerate two-level system for a closed transition $F_g \leftrightarrow F_e = F_g + 1$ with $F_g > 0$ because of the spontaneous transfer of the atomic coherence (TOC),[23] and the dependence of EIA on the field polarization was also discussed. Later Goren

*Project supported by the Natural Science Foundation of the Shanxi Higher Education Institutions of China (Grant No 2007101) and the National Natural Science Foundation of China (Grant No 60708010).
†Corresponding author. E-mail: ybdong@sxu.edu.cn

et al[24] found that EIA can also occur in open systems when the coupling and probe beams have the same polarization rather than a different polarization as in the case of EIA–TOC, and they concluded that this effect is resulted from the EIA–TOP (EIA due to the collision transfer of population (TOP)). But they also considered that EIA takes place for transition $F_g \leftrightarrow F_e = F_g + 1$ with $F_g > 0$. In this paper, the EIA effect is experimentally observed in an open transition $F_g \leftrightarrow F_e = F_g - 1$ ($6^2S_{1/2}$, $F_g = 4 \leftrightarrow 6^2P_{3/2}$, $F_e = 3$ of Cs D_2 Line). Furthermore, an explanation is given with theoretical calculation, which is in good agreement with the experimental results.

With the development of theoretical and experimental investigations, more and more complex quantum coherence effects related to the interactions between multi-field and multi-Zeeman-sublevel systems in the two-level system were developed. The first report about the spectroscopic features of the coherence resonance in the degenerate two-level system showed that the absorption spectra were strongly dependent on the external magnetic field, optical fields' polarization, light intensity, and atomic level characteristics.[21,22] Zeeman coherences are also a basic ingredient of sub-Doppler[25] and sub-recoil[26] laser cooling mechanisms. Later the experimental realization of Gaussian light pulse propagation from subluminal to superluminal based on the transformation from EIT to EIA was obtained in the transition ($6^2S_{1/2}$, $F_g = 4 \leftrightarrow 6^2P_{3/2}$, $F_e = 5$) of Cs D_2 line.[27] The theoretical discussion on the transitions driven by π or $\sigma_\pm$ light and probed by transverse lights with two equal left-handed and right-handed circular polarization components $\sigma_\pm$, showed that the absorption conversion from EIT to EIA and the effects of widening and shifting of EIT windows were investigated.[28–30] All these effects can be considered as a result of the superposition of pure two-level, simple three-level Λ-type and V-type subsystems. Thus for any transition $F_e \leftrightarrow F_g$ with different polarizations of coupling and probe beams, the quantum coherent effects would present various phenomena because different superpositions of the simple energy level configurations are involved. Motivated by this, in this paper, we experimentally and theoretically investigate the quantum effects in the transition $F_g = 4 \leftrightarrow F_e$=3 of the D_2 line of the Cs ensemble with a different combination of the polarization of coupling and probe lights, which results in the different superposition of the V-type, Λ-type, and pure two-level subsystems; thus the absorption properties are greatly modified. A qualitative agreement between experimental results and theoretical calculation is given by using the optical Bloch equation.[24,28,31]

2. Experimental setup and results

A schematic diagram of the experimental setup is shown in Fig.1. Two external cavity diode lasers (ECDL) with less than 1MHz linewidth are used in our measurements. Radiation from the first ECDL used as a pump is locked to the D_2 line transition $6S_{1/2}(F_g = 4) \leftrightarrow 6P_{3/2}(F_e$=3) in Cs^{133}. Radiation from the second ECDL used as a probe is tuned over the transition. At the same time, the frequencies of two lasers are monitored by Doppler-free saturated absorption spectroscopy. Each of the coupling and probe beam passes through an isolator to avoid the light feedback into the lasers. Then after half-wave plates, the two beams with linearly polarizations are combined by a polarizing beam splitter and then sent into the cell with the atomic caesium vapour. Both beams are copropagating and their polarizations are orthogonal to each other. The glass cell ($l = 5$ cm) with atomic caesium vapour at room temperature is placed in a solenoid to control the strength and direction of the magnetic field. A solenoid can produce longitudinal magnetic field (i.e., the quantization axis of magnetic field is perpendicular to the polarization of coupling and probe laser beams), thus both of the coupling and probe beams can be treated as transverse lights with two equal left-handed and right-handed circular polarization components $\sigma_\pm$. After passing through the caesium cell, the probe and coupling beams are separated with another polarizing beam splitter, the probe

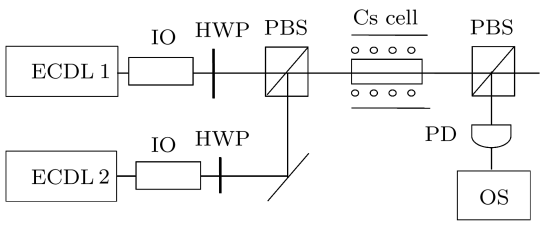


Fig.1. The experimental arrangement. PD: photo detector; ECDL 1 (2): external cavity diode laser 1 (2); IO: isolator; PBS: polarizing beam splitter; HWP: half-wave plate; OS: oscilloscope.

beam is detected by a photodiode and recorded by a digital oscilloscope. The solenoid and the caesium vapour cell are shielded with μ metal sheets to avoid the magnetic field splitting of the sublevels from surrounding magnetic field.

Figure 2 shows a schematic diagram of the partial energy levels for caesium. The Cs D_2 line consists of six allowable optical transitions between either of the two hyperfine ground levels belonging to $6S_{1/2}$ and any of the four hyperfine excited levels belonging to $6P_{3/2}$. So, there are six possible degenerate two-level systems corresponding to each transition. In this paper, we are able to observe EIA in the open and $F_g > F_e$ system, which does not satisfy two conditions among the three EIA conditions.[23] That is to say, we choose the transition $6S_{1/2}(F_g = 4) \leftrightarrow 6P_{3/2}(F_e = 3)$ in Cs as a degenerate two-level system, this is open because decays from the $6P_{3/2}(F_e = 3)$ excited level happen to the ground level $6S_{1/2}(F_g = 3)$, which is not involved in the consideration of a two-level system.

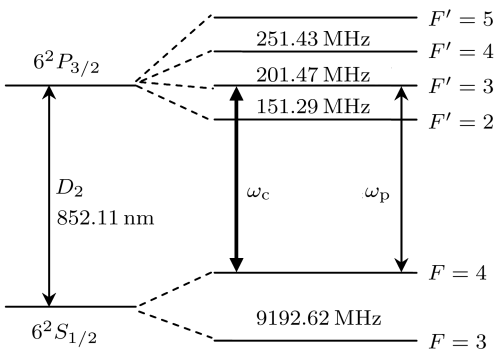


Fig.2. Relevant energy diagram of the Cs D_2 line.

Figure 3 shows the absorption spectra obtained as a function of the probe detuning with different strength of magnetic field B when the atoms are put in a solenoid, the quantization axis of the magnetic field is perpendicular to both the polarization of coupling and probe laser beams, so that both of the linearly polarized coupling and probe lights are decomposed into a left-handed and right-handed circularly polarized component s_+ and s_-. The total Rabi frequencies of the coupling and probe lights are fixed to be $\Omega_c = 28.7\,\mathrm{MHz}$ and $\Omega_p = 9.1\,\mathrm{MHz}$ respectively, which is deduced from the definition about the Rabi frequency of light $\Omega = \Gamma\sqrt{I/2I_0}$; here Γ is the natural decay rate, $I = P/(pr^2)\,\mathrm{mW/cm^2}$ is power density of the field, and the saturation intensity is $I_0 = 1.65\,\mathrm{mW/cm^2}$. The corresponding powers of coupling and the probe beams are $100.3\,\mathrm{mW/cm^2}$ and $10.1\,\mathrm{mW/cm^2}$, respectively. From Figs.3(a)–3(e), the strength of the magnetic field produced by a solenoid is tuned from 0 T up to 1.76×10^{-3} T. As shown in Fig.3(a), the absorption of probe laser shows that the EIA effect is observed for a two-level system when the magnetic field of solenoid is turned off. If a magnetic field is applied, the degeneracy of both the excited and ground levels is broken, and the Zeeman sublevels appear. The involved multilevel coherence modifies the properties of probe absorption. So it is seen from Fig.3(b) that the absorption peak begins to be divided into three peaks. These three EIA peaks are separated and the two absorption peaks at both right and left sides are shifted away from their position with the strength of increasing magnetic field B; on the contrary, the EIA peak in the centre still keeps its position as shown by curves c–e in Figs.3.

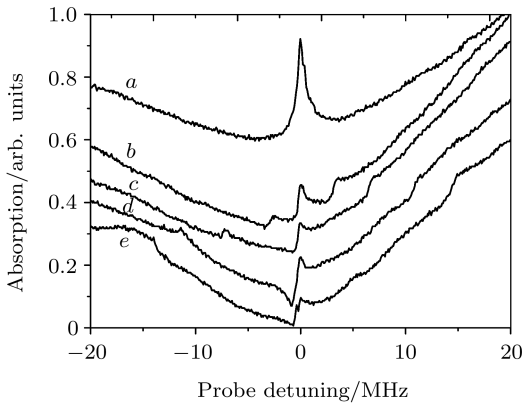


Fig.3. The absorption spectra of the probe beam as a function probe detuning with different magnetic field strength B. The intensity of the coupling and probe lights are $I_c = 100.3\,\mathrm{mW/cm^2}$ and $I_p = 10.1\,\mathrm{mW/cm^2}$. Curve a EIA spectrum with the strength of magnetic field $B = 0$ T. Curves $b - e$ separated and shifted EIA peaks with $B = 4.4 \times 10^{-4}$ T in curve b; $B = 8.8 \times 10^{-4}$ T in curve c; $B = 13.2 \times 10^{-4}$ T in curve d; $B = 17.6 \times 10^{-4}$ T in curve e.

Compared to the sub-MHz laser linewidth, the relatively broad EIA resonances are observed. It is worth mentioning that the EIA spectral line is controlled by the phase coherence of coupling and probe beam while the absolute laser linewidth is less important. To get a narrow EIA spectrum, some techniques have been used to generate mutually coherent laser fields, such as the laser frequency shifting with acousto-optical modulator as demonstrated in Refs.[21,32]. In our system, in order to obtain high power of the coupling beams, two independent ex-

tended cavity diode lasers are used, which is the main reason for the observed broadband EIA signals.

Since the system consisting of $6S_{1/2}(F_{\rm g}=4)$ and $6P_{3/2}(F_{\rm e}=3)$ is open and $F_{\rm g}>F_{\rm e}$, if by Refs.[20–23], EIT would be expected rather than EIA. Absorption spectra should show EIT because the coupling field is pumping atoms optically into other magnetic sublevels uncoupled with the probe field. However, the observed signal is EIA even though it is smaller compared to the closed system $6S_{1/2}(F_{\rm g}=4)\leftrightarrow 6P_{3/2}(F_{\rm e}=5)$.

It should be noted that the experimental results we obtained in Fig.3 show that the absorption peaks are not symmetrical in their heights and positions as we have expected, which are proved to come from the effect of Doppler broadening. We theoretically analyse this effect by introducing a parameter in the term of laser detuning of coupling and probe beams, which explains the reason to break its symmetry. In the following section, we use the optical Bloch equations to qualitatively explain the coherence effects we obtained for the real transition $F_{\rm g}=4\leftrightarrow F_{\rm e}=3$.

3. The theoretical analysis

Figure 4 shows the degenerate two-level system for transition $F_{\rm g}=4\leftrightarrow F_{\rm e}=3$. The Zeeman sublevels of the excited states $6P_{3/2}(F_{\rm e}=3)$ are expressed as $|e_{-3}\rangle$, $|e_{-2}\rangle$, $|e_{-1}\rangle$, $|e_0\rangle$, $|e_1\rangle$, $|e_2\rangle$ and $|e_3\rangle$ for $M_{\rm Fe}=-3$, -2, -1, 0, 1, 2, 3, while the ground states $6S_{1/2}(F_{\rm g}=4)$ are $|g_{-4}\rangle$, $|g_{-3}\rangle$, $|g_{-2}\rangle$, $|g_{-1}\rangle$, $|g_0\rangle$, $|g_1\rangle$, $|g_2\rangle$, $|g_3\rangle$ and $|g_4\rangle$ for $M_{\rm Fg}=-4,-3,-2,-1,0,1,2,3,4$. In the scheme of Fig.4, both of the coupling and probe beams have two equal left-handed and right-handed circular polarized components $\sigma_\pm$. Here the lights with $\sigma_\pm$ polarization interact with the transition $M_{\rm Fe}=i\leftrightarrow M_{\rm Fg}=i\pm1$ ($i=0,\pm1,\pm2,\pm3$). But the system is not closed,

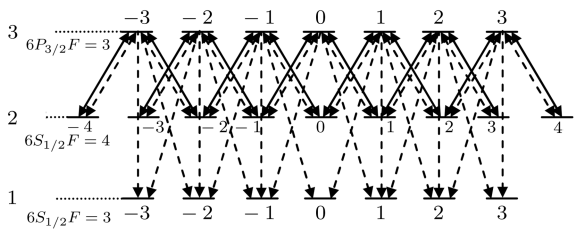


Fig.4. Schematic energy level diagram for a transition $F_{\rm g}=4\leftrightarrow F'_{\rm e}=3\leftrightarrow F_{\rm g}=3$. Solid lines represent the coupling light and dashed lines are for probe field. Both of the coupling and probe lights are circularly $\sigma_\pm$ polarized.

decays from the $6P_{3/2}(F_{\rm e}=3)$ excited level may also happen to the ground level $6S_{1/2}(F_{\rm g}=3)$. As shown in Fig.4, the Zeeman sublevels of the ground states $6S_{1/2}(F_{\rm g}=3)$ are $|g_{-3}\rangle$, $|g_{-2}\rangle$, $|g_{-1}\rangle$, $|g_0\rangle$, $|g_1\rangle$, $|g_2\rangle$ and $|g_3\rangle$ for $M_{\rm Fg}=-3,-2,-1,0,1,2,3$.

We write the evolution equations for the atomic variables as described in Refs.[24,28,31,33],

$$\dot\rho_{ii}^{33}=\frac{\rm i}{\hbar}\sum_k\left(V_{ik}^{32}\rho_{ki}^{23}-\rho_{ik}^{32}V_{ki}^{23}\right)-\Gamma\rho_{ii}^{33},\tag{1}$$

$$\dot\rho_{ij}^{33}=\frac{\rm i}{\hbar}\sum_k\left(V_{ik}^{32}\rho_{kj}^{23}-\rho_{ik}^{32}V_{kj}^{23}\right)-\left({\rm i}\omega_{ij}^{33}+\Gamma\right)\rho_{ij}^{33},\tag{2}$$

$$\dot\rho_{ij}^{32}=\frac{\rm i}{\hbar}\sum_k\left(V_{ik}^{32}\rho_{kj}^{22}-\rho_{ik}^{33}V_{kj}^{32}\right)-\left({\rm i}\omega_{ij}^{32}+\gamma\right)\rho_{ij}^{32},\tag{3}$$

$$\dot\rho_{ii}^{22}=\frac{\rm i}{\hbar}\sum_k\left(V_{ik}^{23}\rho_{ki}^{32}-\rho_{ik}^{23}V_{ki}^{32}\right)-7\Lambda_{21}\rho_{ii}^{22}+\Lambda_{12}\sum_j\rho_{jj}^{11}+\left(\dot\rho_{ii}^{22}\right)_{\rm SE},\tag{4}$$

$$\dot\rho_{ij}^{22}=\frac{\rm i}{\hbar}\sum_k\left(V_{ik}^{23}\rho_{kj}^{32}-\rho_{ik}^{23}V_{kj}^{32}\right)-\left({\rm i}\omega_{ij}^{22}+7\Lambda_{21}\right)\rho_{ij}^{22}+\left(\dot\rho_{ij}^{22}\right)_{\rm SE},\tag{5}$$

$$\dot\rho_{ii}^{11}=-9\Lambda_{12}\rho_{ii}^{11}+\Lambda_{21}\sum_j\rho_{jj}^{22}+\left(\dot\rho_{ii}^{11}\right)_{\rm SE}.\tag{6}$$

Where $\omega_{ij}^{33}=\omega_i^3-\omega_j^3$ and $\omega_{ij}^{22}=\omega_i^2-\omega_j^2$ denote the Zeeman splitting of excited state and ground states, respectively; $\omega_{ij}^{kk}=g_k\mu_{\rm b}B/\hbar(i=j\pm1)$ is the Raman detuning induced by the magnetic field B, where g_k is Lande factor for $k=3$ or 2, and $\mu_{\rm b}$ is the Bohr magnetron; $\omega_{ij}^{32}=\omega_i^3-\omega_j^2$ is transition frequency between excited and ground degenerate levels. Γ is the total spontaneous emission rate from each excited sublevels. $\gamma=(\Gamma+7\Lambda_{21})/2$ is the dephasing rate of excited-state to ground-state coherence, Λ_{21} is the rate of transfer from sublevel $6S_{1/2}(F_{\rm g}=4)$ to $6S_{1/2}(F_{\rm g}=3)$. Λ_{12} is the rate of transfer from sublevel $6S_{1/2}(F_{\rm g}=3)$ to $6S_{1/2}(F_{\rm g}=4)$. $(\dot\rho_{ij}^{mm})_{\rm SE}$ is the spontaneous emission repopulation, which is written as

$$\left(\dot\rho_{ij}^{mm}\right)_{\rm SE}=(2F_3+1)\,\Gamma_{F_3\to F_m}\sum_{p=-1}^{1}\sum_{q,q'=-F_3}^{F_3}(-1)^{p-k-q'}\times\begin{pmatrix}F_m&1&F_3\\-k&p&q\end{pmatrix}\rho_{qq'}^{33}\begin{pmatrix}F_3&1&F_m\\-q'&-p&k'\end{pmatrix},$$

(here, $m=2$ or 1). The dipole moments of transitions are $\mu_{-3-4}^{32}=\mu_{34}^{32}=\mu$, $\mu_{-3-2}^{32}=\mu_{32}^{32}=\sqrt{1/28}\mu$,

$\mu^{32}_{-2-3} = \mu^{32}_{23} = \sqrt{3/4}\mu$, $\mu^{32}_{-2-1} = \mu^{32}_{21} = \sqrt{3/28}\mu$, $\mu^{32}_{-1-2} = \mu^{32}_{12} = \sqrt{15/28}\mu$, $\mu^{32}_{-10} = \mu^{32}_{10} = \sqrt{3/14}\mu$ and $\mu^{32}_{0-1} = \mu^{32}_{01} = \sqrt{5/14}\mu$ for the Cs atom.[34] V^{32}_{ij} is the interaction energy for the transition $|3_i\rangle \leftrightarrow |2_j\rangle$, which is written as

$$V^{32}_{ij} = \hbar V^{32}_{ij}(\omega_{\rm c})\exp(-{\rm i}\omega_{\rm c}t) + \hbar V^{32}_{ij}(\omega_{\rm p})\exp(-{\rm i}\omega_{\rm p}t), \quad (7)$$

($i = 0, \pm1, \pm2, \pm3$, $j = i\pm1$). Of course the magnitudes of $2V^{32}_{ij}(\omega_{\rm p}) = \mu^{32}_{ij}E_{\rm p}/(\sqrt{2}\hbar)$ and $2V^{32}_{ij}(\omega_{\rm c}) = \mu^{32}_{ij}E_{\rm c}/(\sqrt{2}\hbar)$ are the Rabi frequencies of probe and drive fields, respectively. Let $V^{32}_{ij}(\omega_{\rm p})$ and $V^{32}_{ij}(\omega_{\rm c})$ be real for simplicity.

In order to simplify the calculation, we consider the condition that the coupling light is much stronger than the probe light, thus we treat the coupling field to all orders in its Rabi frequency and meanwhile probe the field to first order. Then ρ^{32}_{ij} oscillates at three frequencies:[35,36] the pump frequency $\omega_{\rm c}$, the probe frequency $\omega_{\rm p}$, and the four-wave mixing frequency $2\omega_{\rm c} - \omega_{\rm p}$. We therefore express ρ^{32}_{ij} in terms of its Fourier amplitudes as

$$\rho^{32}_{ij} = \rho^{32}_{ij}(\omega_{\rm c})\exp(-{\rm i}\omega_{\rm c}t) + \rho^{32}_{ij}(\omega_{\rm p})\exp(-{\rm i}\omega_{\rm p}t) + \rho^{32}_{ij}(2\omega_{\rm c} - \omega_{\rm p})\exp[-{\rm i}(2\omega_{\rm c} - \omega_{\rm p})t]. \quad (8)$$

Similarly, the populations and coherences within the same hyperfine level can be written as

$$\rho^{kk}_{ij} = \rho^{kk}_{ij}(dc) + \rho^{kk}_{ij}(\omega_{\rm p} - \omega_{\rm c})\exp[-{\rm i}(\omega_{\rm p} - \omega_{\rm c})t] + \rho^{kk}_{ij}(\omega_{\rm c} - \omega_{\rm p})\exp[-{\rm i}(\omega_{\rm c} - \omega_{\rm p})t]. \quad (9)$$

Where $\rho^{kk}_{ij}(\omega_{\rm p} - \omega_{\rm c})\exp[-{\rm i}(\omega_{\rm p} - \omega_{\rm c})t]$ and $\rho^{kk}_{ij}(\omega_{\rm c} - \omega_{\rm p})\exp[-{\rm i}(\omega_{\rm c} - \omega_{\rm p})t]$ are population and coherence oscillations at frequencies $\omega_{\rm p} - \omega_{\rm c}$ and $\omega_{\rm c} - \omega_{\rm p}$ respectively.

We solve Eqs.(1)–(9) in steady state, for which we set the time derivatives of the Fourier amplitudes equal to zero, and if the relation $\rho_{ij}(\omega_k) = \rho^*_{ji}(-\omega_k)$ is taken into account, these linear equations are readily solved. The probe absorption is calculated from the imaginary part of the susceptibility $\chi(\omega_{\rm p})$, we have

$$\begin{aligned}
&{\rm Im}\chi(\omega_{\rm p}) \\
&\propto {\rm Im}\Big\{\{\mu^{32}_{-3-4}[\rho^{32}_{-3-4}(\omega_{\rm p}) + \rho^{32}_{34}(\omega_{\rm p})] \\
&+\mu^{32}_{-3-2}[\rho^{32}_{-3-2}(\omega_{\rm p}) + \rho^{32}_{32}(\omega_{\rm p})] \\
&+\mu^{32}_{-2-3}[\rho^{32}_{-2-3}(\omega_{\rm p}) + \rho^{32}_{23}(\omega_{\rm p})] \\
&+\mu^{32}_{-2-1}[\rho^{32}_{-2-1}(\omega_{\rm p}) + \rho^{32}_{21}(\omega_{\rm p})] \\
&+\mu^{32}_{-1-2}[\rho^{32}_{-1-2}(\omega_{\rm p}) + \rho^{32}_{12}(\omega_{\rm p})] \\
&+\mu^{32}_{-10}[\rho^{32}_{-10}(\omega_{\rm p}) + \rho^{32}_{10}(\omega_{\rm p})] \\
&+\mu^{32}_{0-1}[\rho^{32}_{0-1}(\omega_{\rm p}) + \rho^{32}_{01}(\omega_{\rm p})]\}/(V^{32}_{0-1}/\gamma)\Big\}. \quad (10)
\end{aligned}$$

In our calculation, we set the driven field detuning to zero, i.e., $\Delta = \omega_{\rm c} - \omega^{32}_{00} = 0$; the probe field detuning is $\delta = \omega_{\rm p} - \omega^{32}_{00}$. We take $\Lambda_{21}/\Gamma = 2.46 \times 10^{-4}$ and $\Lambda_{12}/\Gamma = 1.9 \times 10^{-4}$, which is based on the transferred rate from sublevel $|2_i\rangle$ to $|1_j\rangle$, the transferred rate from sublevel $|1_j\rangle$ to $|2_i\rangle$ and the dephasing rate of the ground-state coherence are smaller than the decay rate from excited to ground state Γ, for the Cs D_2 line, $\Gamma = 5.2\,{\rm MHz}$, i.e., the natural linewidth of Cs D_2 line.[34]

When a magnetic field is present, the Zeeman splitting in the excited and ground states occurs simultaneously, the degeneracy of the two-level system is broken. Note that the Zeeman splitting Δe (or ω^{33}_{10}) of the excited state is not always equal to the splitting Δg (or ω^{22}_{10}) of the ground state. According to the data of Cs atoms for the hyperfine levels of $6S_{1/2}$, $F_{\rm g} = 4$ and $6P_{3/2}$, $F_{\rm e} = 3$, we take $\Delta e = \mu_{\rm B}g_{\rm F}B/\hbar(g_{\rm F} = 0)$ and $\Delta g = \mu_{\rm B}g'_{\rm F}B/\hbar(g'_{\rm F} = 1/4)$. In this case, the total system can be regarded as the superposition of the simple two-level and three-level subsystems, and therefore the quantum coherence shows the complex effects resulted from the superposition of simple subsystems.

The theoretical absorption spectra of the probe beam as a function of the probe detuning for the different strength of magnetic field B are shown in Fig.5. The intensity of the coupling and probe lights are taken to be $V_{\rm c}/\Gamma = V^{32}_{ij}(\omega_{\rm c})/\Gamma = 0.394$, $V_{\rm p}/\Gamma = V^{32}_{ij}(\omega_{\rm p})/\Gamma = 0.125$ ($i = 0, \pm1, \pm2, \pm3$, $j = i \pm 1$). Consider the real transition of $F_{\rm e} = 3 \leftrightarrow F_{\rm g} = 4$, in which there are both fourteen coupling fields $V_{\rm c}$ and probe fields $V_{\rm p}$ interacting with the Zeeman sublevels, thus the total Rabi frequencies of coupling and probe fields ($O_{\rm c}$ and $O_{\rm p}$) are both fourteen times $V_{\rm c}$ and $V_{\rm p}$. ($O_{\rm c} = 14V_{\rm c}$, $O_{\rm p} = 14V_{\rm p}$). The Fig.5(a) is the spectrum of EIA when we take $B = 0$; when a magnetic field is applied. The degeneracy of the two-level system is broken and the Zeeman splitting in the excited and ground states occurs simultaneously. As measured in Fig.3, when the intensity of magnetic field B increases from 0 to 17.6×10^{-4} T, the one EIA peak (Fig.5(a)) obtained from the quantum coherence of degenerate two-level system is broken up into three transparency peaks (Figs.5(b)–5(e)). And it is also shown that the points of the EIA peaks at the right and left sides are shifted its position far from the centre of zero detuning of probe light with the increase of magnetic field, and meanwhile the EIA peak

in the centre does not move its position. This effect of shifting points is the result that the Zeeman splitting increases with the increase of magnetic field, thus the bigger spacing between the two lower levels of Λ-type systems or the two upper level of V-type systems in two-level system leads to the shift of absorption points due to the two-photon resonance of EIA.

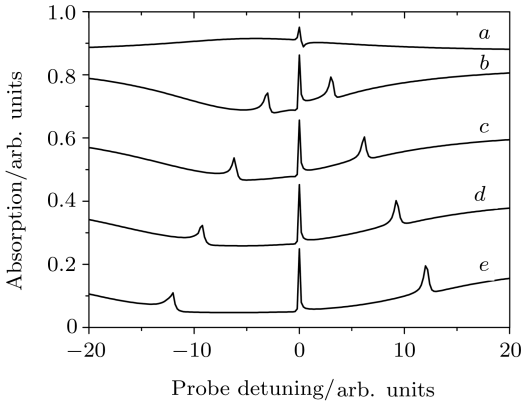


Fig.5. The absorption spectra of the probe beam vs probe detuning with different strength of magnetic field B. Curves a, b, c, d, and e are for $B = 0\,\mathrm{T}$, $4.4 \times 10^{-4}\,\mathrm{T}$, $8.8\times10^{-4}\,\mathrm{T}$, $13.2\times10^{-4}\,\mathrm{T}$, and $17.6\times10^{-4}\,\mathrm{T}$ respectively. Here $k_{\mathrm{p,c}}v = 0.2\Gamma$, the Rabi frequency of the coupling and probe lights are $V_{\mathrm{c}}/\Gamma = 1.138$ and $V_{\mathrm{p}}/\Gamma = 0.175$.

The EIA peaks in Fig.3 are asymmetric, which may come from the effect of Doppler broadening. To take the effect into account, we need to consider the experimental scheme in which the driven and probe beams are copropagating and their frequencies are very close, thus an atom moving towards the driven and probe beams with velocity v_z "sees" their frequencies upshifted by an amount $k_{\mathrm{p,c}}v_z$; here $k_{\mathrm{p,c}}$ is the wave number for the coupling and probe laser, v_z is an averaged velocity averaged over a given velocity distribution $f(v_z)$, which is the Gaussian distribution function of atomic velocities $f(v_z) = (1/v\sqrt{\pi})\exp(-v_z^2/v^2)$. Here we give a qualitative analysis by replacing the detuning $\Delta \Rightarrow \Delta + k_{\mathrm{c}}v$ and $\delta \Rightarrow \delta + k_{\mathrm{p}}v$ with $v \propto \sqrt{\langle v_z^2\rangle}$ and $\langle v_z^2\rangle = \int v_z^2 f(v_z)\mathrm{d}v_z$, where $v = \sqrt{2k_{\mathrm{B}}T/M}$ is the most probable speed of atoms at a given temperature T, M is the atomic mass, and k_{B} is the Boltzmann constant.[37,38] In our numerical discussion, we set $k_{\mathrm{p,c}}v_z = 0.2\Gamma$, with which the calculated curves (see Fig.5) are approximately matched with the experimental results, in which the non-Lorentzian line shapes of EIA peaks are observed; thus we can conclude that the main reason for the asymmetrical EIA resonance comes from the effect of Doppler broadening.

4. Conclusion

In this paper, the quantum coherence in the quasi-degenerate two-level system of transition $F_{\mathrm{e}} = 3 \leftrightarrow F_{\mathrm{g}} = 4$ has been experimentally discussed. The splitting of EIA peak, the shifting and widening of split EIA peaks have been investigated in the presence of magnetic field. These effects are qualitatively explained with the theoretical discussion. The asymmetry of observed spectra has been explained by introducing a laser frequency offset from the optical resonance.

References

[1] Tewari S P and Agarwal G S 1986 *Phys. Rev. Lett.* **56** 1811
[2] Hakuta K, Marmet L and Stoicheff B P 1992 *Phys. Rev.* A **45** 5152
[3] Boller K J, Imamolu A and Harris S E 1991 *Phys. Rev. Lett.* **66** 2593
[4] Shen J Q, Ye J and Zhuang F 2007 *Acta Phys. Sin.* **56** 541 (in Chinese)
[5] Harris S E 1989 *Phys. Rev. Lett.* **62** 1033
[6] Scully M O, Zhu S Y and Gavrielides A 1989 *Phys. Rev. Lett.* **62** 2813
[7] Gray H R, Whitley R M and Stroud Jr C R 1978 *Opt. Lett.* **3** 218
[8] Bi D Y, Cao D M, Cheng Y C, Li Y F, Wang L Q and Zhang C J 2004 *Acta Phys. Sin.* **53** 2937 (in Chinese)
[9] Scully M O 1991 *Phys. Rev. Lett.* **67** 1855
[10] Phillips D F, Fleischhauer A, Mair A, Walsworth R L and Lukin M D 2001 *Phys. Rev. Lett.* **86** 783
[11] Chang H, Li S J, Wang B, Wang H, Wu H B and Xie C D 2005 *Acta Phys. Sin.* **54** 4136 (in Chinese)
[12] Turchette Q A, Hood C J, Lange W, Mabuchi H and Kimble H J 1995 *Phys. Rev. Lett.* **75** 4710
[13] Harris S E and Yamamoto Y 1998 *Phys. Rev. Lett.* **81** 3611
[14] Boto A N, Kok P, Abrams D S, Braunstein S L, Williams C P and Dowling J P 2000 *Phys. Rev. Lett.* **85** 2733
[15] Xiao M, Li Y Q, Jin S Z and Gea-Banacloche J 1995 *Phys. Rev. Lett.* **74** 666
[16] Li Y Q and Xiao M 1995 *Phys. Rev.* A **51** R2703
[17] Moseley R R, Shepherd S, Fulton D J, Sinclair B D and Dunn M H 1995 *Phys. Rev. Lett.* **74** 670
[18] Dong Y B, Gao J R, Wang H H and Zhang J X 2006 *Chin. Phys.* **15** 1262
[19] Dong Y B, Wang H H, Gao J R and Zhang J X 2006 *Phys. Rev.* A **74** 063810

[20] Lezama A, Barreiro S and Akulshin A M 1999 *Phys. Rev.* A **59** 4732
[21] Lezama A, Barreiro S, Lipsich A and Akulshin A M 1999 *Phys. Rev.* A **61** 013801
[22] Lipsich A, Barreiro S, Akulshin A M and Lezama A 2000 *Phys. Rev.* A **61** 053803
[23] Akulshin A M, Barreiro S and Lezama A 1999 *Phys. Rev. Lett.* **83** 4277
[24] Goren C, Wilson-Gordon A D, Rosenbluh M and Friedmann H 2003 *Phys. Rev.* A **67** 033807
[25] Dalibard J and Cohen-Tannoudji C 1989 *J. Opt. Soc. Am.* B **6** 2023
[26] Aspect A, Arimondo E, Kaiser R, Vansteenkiste N and Cohen-Tannoudji C 1988 *Phys. Rev. Lett.* **61** 826
[27] Kim K, Moon H S, Lee C, Kim S K and Kim J B 2003 *Phys. Rev.* A **68** 013810
[28] Gu Y, Sun Q Q and Gong Q H 2003 *Phys. Rev.* A **67** 063809
[29] Gu Y, Sun Q Q and Gong Q H 2004 *J. Phys.* B **37** 1553
[30] Sun Q Q, Gu Y and Gong Q H 2004 *J. Mod. Opt.* **51** 1899
[31] Ling H Y, Li Y Q and Xiao M 1996 *Phys. Rev.* A **53** 1014
[32] Akulshin A M, Barreiro S and Lezama A 1998 *Phys. Rev.* A **57** 2996
[33] Renzoni F, Maichen W, Windholz L and Arimondo E 1997 *Phys. Rev.* A **55** 3710
[34] Steck D A 2003 http://steck.us/alkalidata
[35] Wilson-Gordon A D and Friedmann H 1983 *Opt. Lett.* **8** 617
[36] Boyd R W, Raymer M G, Narum P and Harter D J 1981 *Phys. Rev.* A **24** 411
[37] Wu Y and Yang X X 2005 *Phys. Rev.* A **71** 053806
[38] Ye C Y, Rostovtsev Y V, Zibrov A S and Golubev Y M 2002 *Opt. Commun.* **207** 227